Studies on the magnetic and structural phase transitions of Nd_3RuO_7

2001 J. Phys.: Condens. Matter 13 10825

(http://iopscience.iop.org/0953-8984/13/48/308)

INSTITUTE OF PHYSICS PUBLISHING JOURNAL OF PHYSICS: CONDENSED MATTER

J. Phys.: Condens. Matter **13** (2001) 10825–10836 PII: S0953-8984(01)22896-3

Studies on the magnetic and structural phase transitions of Nd_3RuO_7

Daijitsu Harada[1], **Yukio Hinatsu**[1] **and Yoshinobu Ishii**[2]

[1] Division of Chemistry, Graduate School of Science, Hokkaido University, Sapporo 060-0810, Japan
[2] Japan Atomic Energy Research Institute, Tokai-mura, Ibaraki 319-1195, Japan

Received 15 March 2001, in final form 1 August 2001
Published 16 November 2001
Online at stacks.iop.org/JPhysCM/13/10825

Abstract

Crystal structures and magnetic and thermal properties of neodymium ruthenate Nd_3RuO_7 have been investigated. The specific heat and neutron diffraction measurements showed a monoclinic–orthorhombic structural phase transition at 130 K. The monoclinic crystal structure at 100 K is well described with the space group $P2_1/m$ ($a = 10.8893(4)$ Å, $b = 7.3864(2)$ Å, $c = 7.4731(2)$ Å and $\beta = 90.008(6)^\circ$). The results of the magnetic susceptibility measurements show the existence of the antiferromagnetic transition with a weak ferromagnetic component at 19 K. Specific heat and neutron diffraction measurements also indicated long-range magnetic ordering of both Nd^{3+} and Ru^{5+} ions below 19 K. The magnetic sublattice of Nd^{3+} ions was twice as large as the size of the crystal lattice along the *b*-axis. On the other hand, the size of the magnetic sublattice of Ru^{5+} was the same as that of the crystal lattice. Ru^{5+} ions were coupled anti-ferromagnetically along the *c*-axis.

1. Introduction

Recently, ruthenium-based oxides with a fluorite-related structure Ln_3RuO_7 (Ln = lanthanides) have been studied extensively [1–7]. They are part of a large family of chain compounds with the formula Ln_3MO_7 (M = pentavalent 4d, 5d transition metal cations). The M^{5+} cation is octahedrally coordinated and the octahedra share corners forming a zig-zag chain parallel to the *c*-axis. The interchain M–M distance is about 6.6 Å compared with the corresponding intra-chain distance of 3.7 Å, which suggests that these compounds may exhibit one-dimensional electronic behaviour. A variety of the space groups has been proposed for the Ln_3MO_7. For the irridinates, *Cmcm* appears to provide a good description [8], while for M = Nb and Mo, *Pnma* [9] and $P2_12_12_1$ [10] have been adopted, respectively.

The crystal structure of Ln_3RuO_7 (Ln = La, Pr, Nd–Gd) is well described in space group *Cmcm*. In this structure, slabs are formed in the *bc*-plane, in which a one-dimensional RuO_6 chain runs parallel to the *c*-axis alternating with rows of edge-shared LnO_8 pseudo cubes consisting of one-third of Ln ions. These slabs are separated by the remaining two-thirds of Ln ions which is seven-coordinated by oxygen ions. These compounds show

magnetic transitions at low temperatures, i.e. at 14.5–23 K for Ln_3RuO_7 (Ln = La, Sm–Gd) [3, 6, 7] and at 50 K for Pr_3RuO_7 [5]. For Sm_3RuO_7 and Gd_3RuO_7, another magnetic anomaly due to the ordering of Ru^{5+} and Ln^{3+} ions has been observed [6, 7].

In the present study, we focus our attention on a neodymium ruthenate Nd_3RuO_7 which belongs to the same Ln_3RuO_7 system. Previously, we reported the magnetic and thermal properties of Ln_3RuO_7 (Ln = Sm, Eu) [7]. Through their specific heat measurements, we have found structural phase transitions for Ln_3RuO_7 (Ln = Sm, Eu) at 190 and 280 K, respectively. For Nd_3RuO_7, similar crystal phase transition is expected to occur at low temperatures because the crystal structure of this compound at room temperature is described with space group *Cmcm*, which is the same for the case of Sm_3RuO_7 and Eu_3RuO_7. In Nd_3RuO_7, there exist two kinds of magnetic ions, Nd^{3+} and Ru^{5+}. The electronic structure of Nd^{3+} and Ru^{5+} is $[Xe]4f^3$ ([Xe]: xenon electronic core) and $[Kr]4d^3$ ([Kr]: krypton electronic core), respectively. So, both the cations should greatly contribute to the magnetic properties of this compound. To elucidate these points we have studied its crystal structure at low temperatures and magnetic and thermal properties through neutron diffraction, magnetic susceptibility and specific heat measurements.

2. Experimental

A polycrystalline sample of Nd_3RuO_7 was synthesized by heating a stoichiometric amount of Nd_2O_3 and RuO_2 in air at 1200 °C for 48 h with frequent grindings. A powder x-ray diffraction (XRD) pattern was measured with Cu K_α radiation on a Multi Flex (Rigaku) diffractometer. XRD data were collected by the step scanning over the range $10° \leqslant 2\theta \leqslant 120°$ in increments of $0.02° (2\theta)$.

Powder neutron diffraction measurements were performed at 100 and 10 K using a high resolution powder diffractometer (HRPD) at the JRR-3M reactor (Japan Atomic Energy Research Institute), with a Ge(331) monochromator ($\lambda = 1.823$ Å) in the range $0.05° \leqslant 2\theta \leqslant 165°$ at intervals of 0.05 ° [11]. The collimators used were 6′-20′-6′, which were placed before and after the monochromator and between the sample and each detector. The set of 64 detectors and collimators, which were placed every 2.5 °, rotates around the sample. The crystal and magnetic structures were determined by the Rietveld technique using the Rietan-2000 program [12].

The temperature dependence of the magnetic susceptibility on Nd_3RuO_7 was measured for Nd_3RuO_7 over the temperature region $2\ K \leqslant T \leqslant 300\ K$ in a magnetic field of 0.1 T with SQUID magnetometer (Quantum Design, Model MPMS). The magnetic susceptibility data were collected both after cooling the sample from room temperature to 2 K in a zero field cooling (ZFC) and after field cooling (FC) it in an applied field of 0.1 T. The field-dependence of magnetization was measured at 5 K over the applied magnetic field range $-5\ T \leqslant H \leqslant 5\ T$.

The temperature dependence of the specific heat was performed using a relaxation technique for Nd_3RuO_7 in the temperature range $1.8 \leqslant T \leqslant 300$ K. The sample in the form of a pellet was mounted on an aluminum plate with apiezon for better thermal contact. Measurements of specific heat were recorded with Quantum Design, PPMS.

3. Results and discussion

3.1. X-ray diffraction measurement

The crystal structure is analysed to be orthorhombic with the space group *Cmcm* at room temperature, which accords with the result reported previously for Ln_3RuO_7 [1, 2]. Table 1

Table 1. Crystal and magnetic structure data for Nd_3RuO_7[a].

Atoms	Site	x	y	z	B (Å^2)
X-ray diffraction measurements at RT					
space group $Cmcm$ (No 63) $Z = 4$					
$a = 10.9043(5)$ Å, $b = 7.3811(3)$ Å, $c = 7.4955(3)$ Å, $V = 603.29(4)$ Å^3					
$R_{wp} = 14.23\%$, $R_e = 11.03\%$, $R_I = 2.10\%$					
Nd(1)	4a	0.0	0.0	0.0	0.74(5)
Nd(2)	8g	0.2223(1)	0.3094(1)	0.25	0.25(3)
Ru	4b	0.0	0.5	0.0	0.04(5)
O(1)	16h	0.124(1)	0.318(1)	−0.039(1)	0.60(15)
O(2)	8g	0.130(1)	0.029(1)	0.25	0.60(15)
O(3)	4c	0.0	0.423(2)	0.25	0.60(15)
Neutron diffraction measurements at 100 K					
space group $P2_1/m$ (No 11) $Z = 4$					
$a = 10.8893(4)$ Å, $b = 7.3864(2)$ Å, $c = 7.4731(2)$ Å, $\gamma = 90.008(6)^\circ$, $V = 601.07(3)$ Å^3					
$R_{wp} = 11.66\%$, $R_e = 10.23\%$, $R_I = 4.40\%$					
Nd(1)	2a	0.0	0.0	0.0	1.47(10)
Nd(2)	2d	0.5	0.5	0.0	1.47(10)
Nd(3)	2e	0.217(2)	0.308(2)	0.25	0.37(7)
Nd(4)	2e	0.776(2)	0.310(2)	0.25	0.37(7)
Nd(5)	2e	0.727(2)	0.811(2)	0.25	0.37(7)
Nd(6)	2e	0.276(2)	0.806(2)	0.25	0.37(7)
Ru(1)	2b	0.0	0.5	0.0	0.84(10)
Ru(2)	2c	0.5	0.0	0.0	0.84(10)
O(1)	2e	−0.010(2)	0.400(2)	0.25	0.23(16)
O(2)	2e	0.505(3)	0.930(2)	0.25	0.23(16)
O(3)	2e	0.131(3)	0.027(3)	0.25	0.77(9)
O(4)	2e	0.866(3)	0.038(3)	0.25	0.77(9)
O(5)	2e	0.632(2)	0.527(3)	0.25	0.77(9)
O(6)	2e	0.371(3)	0.523(3)	0.25	0.77(9)
O(7)	4f	0.113(2)	0.293(2)	−0.037(3)	1.17(9)
O(8)	4f	0.855(3)	0.358(2)	−0.047(2)	1.17(9)
O(9)	4f	0.624(3)	0.816(2)	−0.042(3)	1.17(9)
O(10)	4f	0.377(2)	0.812(2)	−0.041(3)	1.17(9)

lists the lattice parameters and the atomic positions for Nd_3RuO_7 refined by the Rietveld analysis. The lattice parameters are determined to be $a = 10.9043(5)$ Å, $b = 7.3811(3)$ Å and $c = 7.4955(3)$ Å. These lattice parameters and atomic positions are in good agreement with those determined by powder neutron diffraction measurements [2].

3.2. Magnetic properties

The temperature dependence of the molar magnetic susceptibilities for Nd_3RuO_7 is shown in figure 1. The susceptibility increases rapidly with decreasing temperature through ca 25 K and ZFC susceptibility shows antiferromagnetic transition at 19 K. Dramatic divergence between the ZFC and FC susceptibilities is observed below the Néel temperature. A maximum in the FC susceptibility appears at ca 15 K. The magnetic hysteresis loop is observed in the field-dependence of the magnetization curve (see figure 2) indicating the existence of a ferromagnetic component. It is estimated to be $\mu = 0.24\ \mu_B$ from the remnant magnetization. When the magnetic field of 5 T is applied, the magnetic moment of Nd_3RuO_7 is 3.07 μ_B. In

Table 1. (*Continued*)

Atoms	Site	x	y	z	B (Å^2)
Neutron diffraction measurements at 10 K					
space group $P2_1/m$ (No 11) $Z = 4$					
$a = 10.8846(3)$ Å, $b = 7.3907(2)$ Å, $c = 7.4679(2)$ Å, $\gamma = 90.008(5)^\circ$, $V = 600.75(3)$ Å^3					
$R_{wp} = 10.25\%$, $R_e = 7.54\%$, $R_I = 5.05\%$					
Nd(1)	2a	0.0	0.0	0.0	1.23(9)
Nd(2)	2d	0.5	0.5	0.0	1.23(9)
Nd(3)	2e	0.228(1)	0.316(2)	0.25	0.31(7)
Nd(4)	2e	0.775(1)	0.306(2)	0.25	0.31(7)
Nd(5)	2e	0.720(1)	0.808(2)	0.25	0.31(7)
Nd(6)	2e	0.278(1)	0.810(2)	0.25	0.31(7)
Ru(1)	2b	0.0	0.5	0.0	1.00(9)
Ru(2)	2c	0.5	0.0	0.0	1.00(9)
O(1)	2e	0.002(2)	0.434(1)	0.25	0.46(14)
O(2)	2e	0.491(2)	0.903(2)	0.25	0.46(14)
O(3)	2e	0.139(2)	0.030(3)	0.25	0.79(8)
O(4)	2e	0.872(2)	0.028(3)	0.25	0.79(8)
O(5)	2e	0.631(2)	0.521(3)	0.25	0.79(8)
O(6)	2e	0.369(2)	0.539(3)	0.25	0.79(8)
O(7)	4f	0.127(1)	0.321(1)	−0.038(3)	0.98(7)
O(8)	4f	0.880(1)	0.313(2)	−0.036(3)	0.98(7)
O(9)	4f	0.609(1)	0.786(2)	−0.046(2)	0.98(7)
O(10)	4f	0.351(1)	0.861(1)	−0.048(1)	0.98(7)

[a] *Note*. Definitions of reliability factors R_{wp}, R_e and R_I are given as follows: $R_{wp} = [\sum_i w_i(y_i - f_i(\mathbf{x}))^2 / \sum_i w_i y_i^2]^{1/2}$, $R_e = [N_o - N_r - N_c / \sum_i w_i y_i^2]^{1/2}$ and $R_\mathrm{I} = [\sum_k |I_k(\mathrm{obs}) - I_k(\mathrm{calc})| / \sum_k I_k(\mathrm{obs})]$.

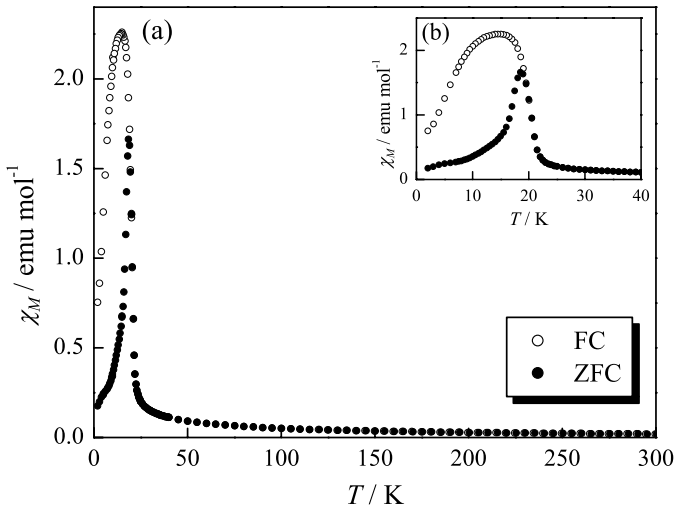

Figure 1. Temperature dependence of magnetic susceptibility for Nd_3RuO_7 in the temperature ranges (a) $2 \leqslant T \leqslant 300$ K and (b) $2 \leqslant T \leqslant 40$ K.

the case when all magnetic ions in Nd_3RuO_7, i.e. three Nd^{3+} and one Ru^{5+} ions per formula unit are ferromagnetically arranged, the theoretically ordered moment is $\mu = 12.8\ \mu_\mathrm{B}$. The observed moment is smaller than this value. Therefore, we conclude that Nd_3RuO_7 is antiferromagnetically coupled with a weak ferromagnetic component.

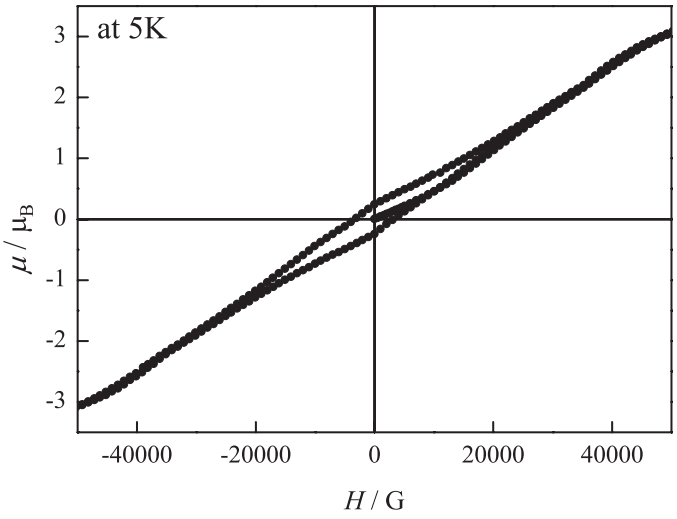

Figure 2. Magnetic field dependence of magnetization of Nd_3RuO_7 at 5 K.

We estimate an effective magnetic moment (μ_{eff}) and a Weiss constant (θ) in the temperature range $100 < T < 300$ K in which the Currie–Weiss law holds. The observed effective magnetic moment is determined to be 7.24 μ_B. The effective magnetic moment expected for Nd_3RuO_7 is calculated to be 7.37 μ_B by substituting the theoretical free-ion magnetic moments, $\mu_{Nd^{3+}} = 3.62\ \mu_B$ and $\mu_{Ru^{5+}} = 3.87\ \mu_B$ into the following equation, $\mu_{Nd_3RuO_7} = \sqrt{3\mu_{Nd^{3+}} + \mu_{Ru^{5+}}}$. The observed moment is close to the theoretical moment of Nd_3RuO_7. We consider that a little difference in the moment may come from the crystal field splitting of the ground state of Nd^{3+} and/or Ru^{5+} ions. The Weiss constant is estimated to be $\theta = -26$ K. This negative value corresponds to the antiferromagnetic interactions found in Nd_3RuO_7.

3.3. Thermal properties

Figure 3 shows the variation of specific heat for Nd_3RuO_7 as a function of temperature. Three thermal anomalies have been observed. The λ-type anomaly at 19 K corresponds to the magnetic transition observed in the susceptibility measurements. This magnetic transition temperature is close to those for La_3RuO_7 (17 K) and Eu_3RuO_7 (22.5 K) in which lanthanide ions are nonmagnetic and only ruthenium ions are magnetic. The fact that the transition temperatures are comparable implies that the magnetic transition at 19 K for Nd_3RuO_7 is due to the magnetic interactions between Ru^{5+} ions. For Nd_3RuO_7, the other two thermal anomalies have been observed at 5 and 130 K.

We will estimate the magnetic entropy change associated with the antiferromagnetic interactions from the specific data. To calculate the magnetic contribution to the specific heat, we have to subtract electronic and lattice contributions from the total specific heat. In figure 3, the specific heat data for the diamagnetic La_3NbO_7 which is isomorphous with Nd_3RuO_7 are also shown. If we assume that the electronic and lattice contributions to the specific heat between Nd_3RuO_7 and La_3NbO_7 are equal, the magnetic specific heat for Nd_3RuO_7 is obtained by subtracting the specific heat of La_3NbO_7. Figure 4 shows the magnetic specific heat of Nd_3RuO_7 divided by temperature as a function of temperature. A dashed line represents the extrapolated magnetic specific heat below 1.8 K. This is calculated by fitting the magnetic specific heat to the function $f(T) = a \times T^3$ in the temperature ranges $1.8 < T < 3.0$ K. The

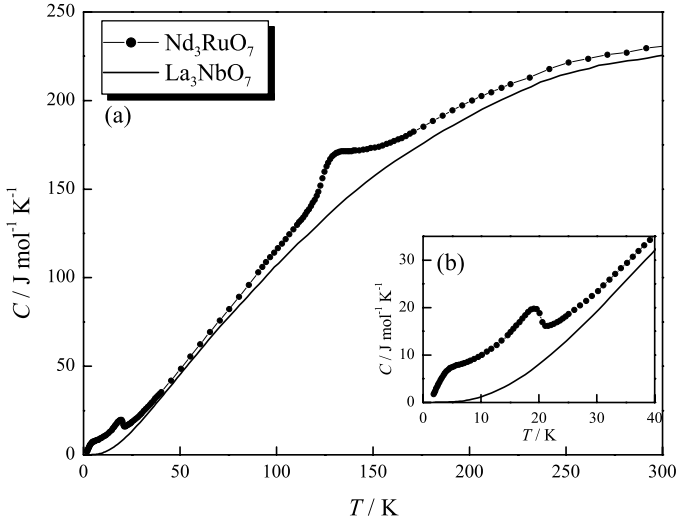

Figure 3. Temperature dependence of specific heat of Nd_3RuO_7 in the temperature ranges (a) $1.8 \leqslant T \leqslant 300$ K and (b) $1.8 \leqslant T \leqslant 40$ K. The specific heat of La_3NbO_7 is shown with a solid line.

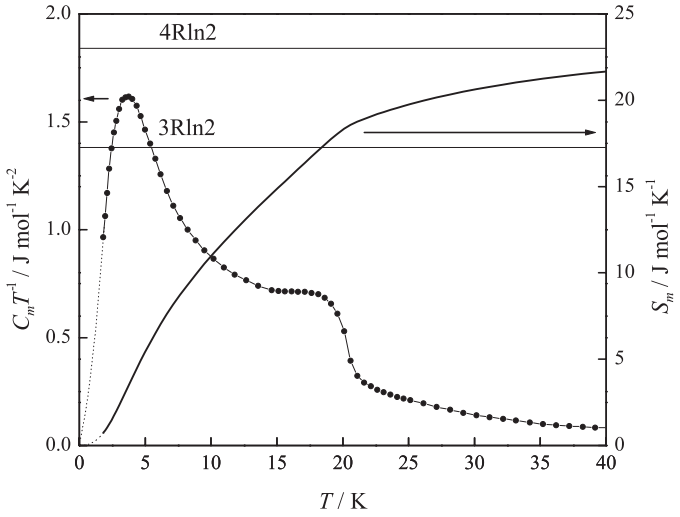

Figure 4. The C_m/T (left ordinate) versus temperature and the magnetic entropy change (right ordinate) versus temperature for Nd_3RuO_7.

magnetic entropy change associated with the antiferromagnetic transition is calculated to be 21.6 J mol^{-1} K^{-1} (at 300 K) by integrating $S_m(T) = \int (C_m/T)\,\mathrm{d}T$. This value is close to $4R\ \ln(2S+1) = 4R\ \ln(2\frac{1}{2}+1) = 23.04$ J mol^{-1} K^{-1} (see figure 4), where R is a molar gas constant and S is a total spin quantum number.

Previously we reported the magnetic entropy change for the antiferromagnetic alignment of Eu_3RuO_7 and Sm_3RuO_7 [7]. Although a total spin quantum number of Ru^{5+} is calculated to be $S = 3/2$ for these compounds, the four degenerating states split into two doublets $|S = 3/2,\ M_S = \pm 3/2\rangle$ and $|S = 3/2,\ M_S = \pm 1/2\rangle$. Therefore, we concluded that the magnetic entropy change of Ru^{5+} ions in these compounds is $R \ln 2$. When the same estimation for the magnetic entropy change of Ru^{5+} ions holds for the case of Nd_3RuO_7, the rest of the magnetic entropy change $3R\ \ln 2$ is due to the Nd^{3+} ions. It means that Nd^{3+} ions as well as Ru^{5+}

ions cause magnetic ordering below magnetic transition temperature. Low symmetry of the oxygen-coordination around the Nd^{3+} site distorts its crystal electric field, implying that the ground state of Nd^{3+} should be a Kramers' doublet. In the case when three Kramers' ions order, the expected magnetic entropy change is $3R$ ln 2, which accords with the estimated value. A slight inflection is found at ca 6 K in the magnetic entropy versus temperature curve (figure 1), which corresponds to the maximum in the C_m/T versus T curve (figure 4). This fact indicates that the ordering of magnetic moment of Nd^{3+} proceeds rapidly below this temperature. However, the magnetic entropy change due to Nd^{3+} ions still continues above this inflection temperature. Therefore, it seems that Nd^{3+} ions magnetically order when the temperature decreases to 19 K. A similar magnetic entropy versus temperature curve has been observed for Sm_3RuO_7 [7] and it has a more prominent inflection at ca 10 K (below the transition temperature, 22.5 K) compared with that for Nd_3RuO_7.

Another specific heat anomaly is observed at 130 K, indicating the occurrence of the first-order transition at this temperature. The first-order transition was also observed for Sm_3RuO_7 (190 K) and Eu_3RuO_7 (280 K) [7]. By increasing the atomic number of lanthanides, the shape of this anomaly becomes broader and the transition temperature remains lower. These systematic changes indicate that this transition is the structural phase transition. This structural phase transition for Nd_3RuO_7 will be discussed below in detail with the results of its neutron diffraction measurements.

3.4. Neutron diffraction

Neutron diffraction measurements were performed at 100 and 10 K. For the diffraction data, we first attempted to refine the crystal structure with the space group *Cmcm* which is the same space group as at room temperature. However, some weak peaks which could not be indexed, appeared at 100 K and the reliability factor was not good. The analysis with the space group $P2_1/m$ gives better results than those with the space group *Cmcm*. Figure 5 shows the diffraction profile in the range of $100^\circ \leqslant 2\theta \leqslant 120^\circ$ and its Rietveld fittings. The neutron diffraction measurements and their analysis indicate that the crystal structure at 100 K is monoclinic with space group $P2_1/m$, i.e. the monoclinic–orthorhombic crystal phase transition occurs between 100 K and room temperature. The lattice parameters at 100 K are determined as $a = 10.8893(4)$ Å, $b = 7.3864(2)$ Å, $c = 7.4731(2)$ Å and $\gamma = 90.008(6)^\circ$. Note that we use the *c*-unique setting for the monoclinic phase. The specific heat anomaly observed at ca 130 K corresponds to this monoclinic–orthorhombic structural phase transition. Figure 6 shows the crystal structure of Nd_3RuO_7 at 100 K. In this figure, we compare it with the structure at room temperature. Table 2 lists some selected bond lengths and angles for Nd_3RuO_7 at 100 K and room temperature. In the crystal structure at room temperature, one-dimensional RuO_6 chain tilts in the *bc*-plane, while at 100 K, half of this chain tilts in the *ab*-plane as well as in the *bc*-plane. Therefore, half of the NdO_8 pseudo-cubes sharing edge with RuO_6 octahedra at room temperature change into NdO_6 octahedra sharing corner with RuO_6 octahedra at 100 K. This structural change accompanies the shift of oxygen ions away from Nd^{3+} ions along the *b*-axis. The Nd–O bond length 2.75 Å which is included in the NdO_8 pseudo-cube at room temperature (Nd(1)–O(1) with space group *Cmcm*) extends to 3.10 Å at 100 K (Nd(1)–O(8) with space group $P2_1/m$). From Shannon's ionic radii, the eight-coordinated Nd–O bond length is calculated to be 2.489 Å. Therefore, the O(8) at a distance of 3.10 Å from the Nd(1) does not form the coordination polyhedron. This oxygen shift is the most remarkable change through structural phase transition and it occurs almost along the *b*-axis, which results in the longer *b* lattice parameter at 100 K than that at room temperature.

Figure 7 shows the neutron diffraction profile measured at 10 K. A lot of magnetic reflections are observed in a low diffraction-angle range, which means that magnetic long-range

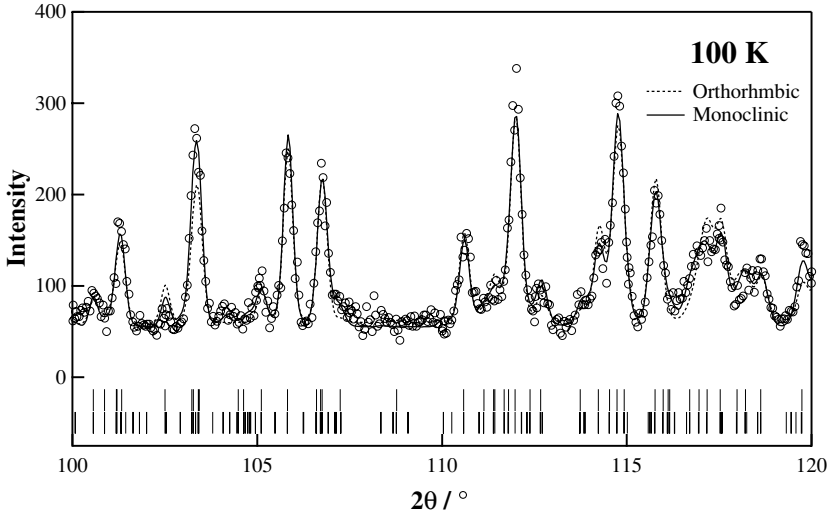

Figure 5. Neutron diffraction profile for Nd_3RuO_7 at 100 K in the range of $100^\circ \leqslant 2\theta \leqslant 120^\circ$. The Reitveld fittings were performed with the space groups $P2_1/m$ (monoclinic phase) and *Cmcm* (orthorhombic phase). The vertical marks on the bottom show the positions calculated for Bragg reflections.

ordering exists at this temperature. This result corresponds to the susceptibility and specific heat results which show magnetic transition at 19 K. Some of the magnetic diffraction peaks are indexed with $(x, 1/2, z)$, which indicates that the magnetic lattice is twice as large as the crystal lattice along the *b*-axis. In Nd_3RuO_7, both Nd^{3+} and Ru^{5+} ions order and form the magnetic sublattice. Considering that the magnetic transitions of La_3RuO_7 and Eu_3RuO_7 have been observed at 17 and 22.5 K, respectively, we believe the magnetic transition observed at 19 K for this Nd_3RuO_7 is also due to interactions between Ru^{5+} ions. The magnetic diffraction of the Ru^{5+} sublattice should contribute to the magnetic reflection peak (1 0 1) (0 1 1) with the strongest intensity in the neutron diffraction profile measured at 10 K. We have found that any model of the Ru^{5+} sublattice with the double magnetic size compared with the size of its crystal lattice, is not acceptable for the present case. Therefore, we expect that the magnetic sublattice of Nd^{3+} ions is twice as large as that of the size of crystal lattice and that the magnetic sublattice of Ru^{5+} ions is as large as the crystal lattice.

First, we will consider the magnetic structural model for the Ru^{5+} sublattice. In the monoclinic space group $P2_1/m$, with Ru^{5+} ions at the 2b and 2c Wyckoff's positions, following four magnetic sites are available for the Ru^{5+} ions:

Ru1: (0, 0.5, 0),
Ru2: (0, 0.5, 0.5),
Ru3: (0.5, 0, 0),
Ru4: (0.5, 0, 0.5),

with respective magnetic moments S_1, S_2, S_3 and S_4. Four types of magnetic arrangement are possible:

Model I: $S_1 + S_2 + S_3 + S_4$,
Model II: $S_1 + S_2 - S_3 - S_4$,
Model III: $S_1 - S_2 + S_3 - S_4$,
Model IV: $S1 - S_2 - S_3 + S_4$,

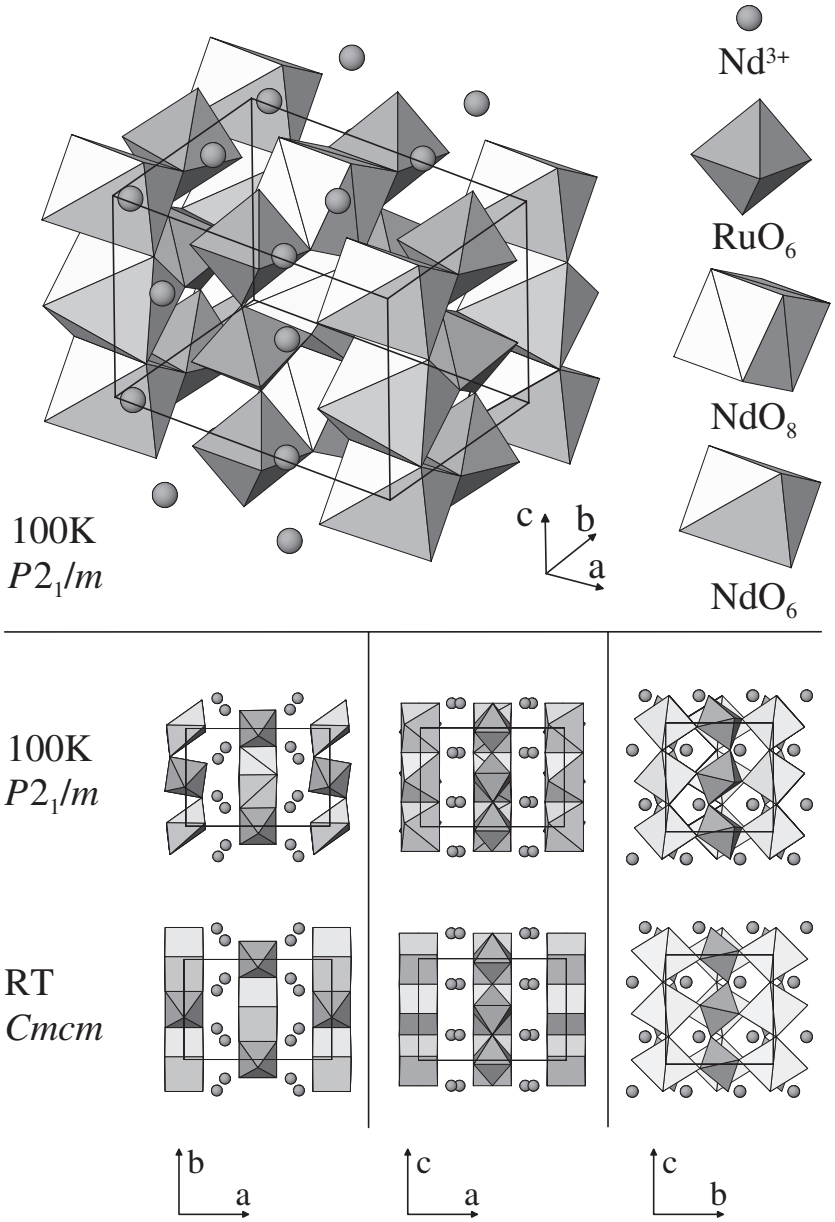

Figure 6. The crystal structure of Nd_3RuO_7 at 100 K compared with that at room temperature.

where the arrangement for model I is ferromagnetic and those for the other models are antiferromagnetic. The magnetic structure factor $Fm(h\,k\,l)$ for an $(h\,k\,l)$ reflection is given by the following equation:

$$F_m = \sum_j q_j b_m \exp 2\pi \mathrm{i}(hx_j + ky_j + lz_j). \tag{1}$$

Table 2. Selected bond lengths (Å) and angles (°) for Nd_3RuO_7.

	Average	
RT		
Nd(1)–O (8-coordination)		
2.351 × 4 2.747 × 4	2.55	
Nd(2)–O (7-coordination)		
2.281 2.323 2.412 × 2 2.475 × 2 2.560	2.42	
Ru(1)–O (6-coordination)		
1.9382 × 4 1.9631 × 2	1.95	
Ru–O–Ru		
145.33		
100 K		
Nd(1)–O (6-coordination)		
2.3577 × 2 2.3890 × 2 2.5028 × 2	2.42	
Nd(2)–O (8-coordination)		
2.3449 × 2 2.3661 × 2 2.6864 × 2 2.7149 × 2	2.53	
Nd(3)–O (7-coordination)		
2.2885 2.2979 2.4349 × 2 2.4928 × 2 2.5718	2.43	
Nd(4)–O (7-coordination)		
2.2341 2.2440 2.3995 × 2 2.4202 2.4572 × 2	2.37	Average of 7-coordinated Nd–O
Nd(5)–O (7-coordination)		2.41
2.2464 2.3486 2.4525 × 2 2.4828 × 2 2.5787	2.43	
Nd(6)–O (7-coordination)		
2.2752 2.3280 2.4109 × 2 2.4361 × 2 2.6481	2.42	
Ru(1)–O (6-coordination)		
1.9384 × 2 1.9460 × 2 1.9536 × 2	1.95	Average of 6-coordinated Ru–O
Ru(2)–O (6-coordination)		1.95
1.9384 × 2 1.9460 × 2 1.9536 × 2	1.95	
Ru–O–Ru		
136.73		
Calculated bond lengths from Shannon's ionic radius		
6-coordinated Ru–O	1.945	
6-coordinated Nd–O	2.363	
8-coordinated Nd–O	2.489	

The magnetic reflection conditions for each magnetic arrangement are as follows:

	$h+k$	l
Model I	Even	Even
Model II	Odd	Even
Model III	Even	Odd
Model VI	Odd	Odd

The (1 0 0) and (0 0 1) magnetic reflections are absent in the profile of Nd_3RuO_7 and the clear enhancements of peak intensities for (1 0 1) and (0 1 1) reflections are recognized in the pattern at 10 K compared with that at 100 K. Following this reflection condition rule, we have concluded that the model IV magnetic arrangement is appropriate for the Ru^{5+} sublattice. The schematic magnetic structure of Ru^{5+} sublattice is illustrated in figure 8, showing that the Ru^{5+} ions are coupled anti-ferromagnetically in one-dimensional chains along the *c*-axis.

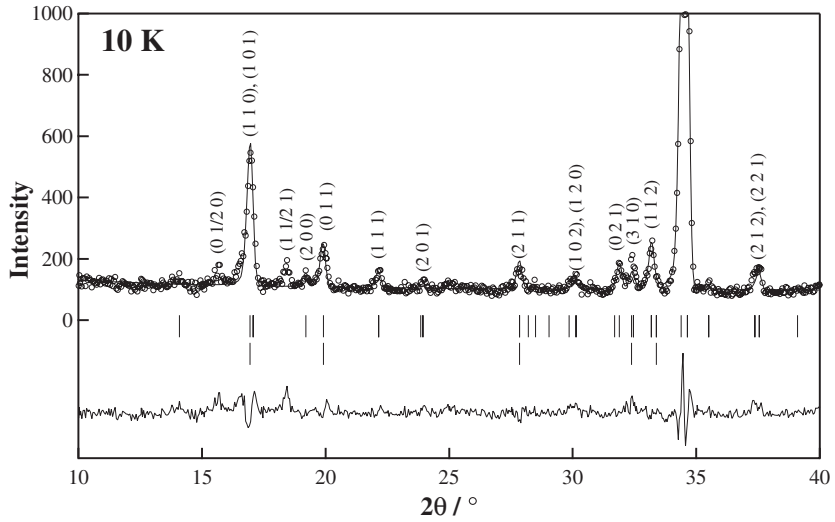

Figure 7. Neutron diffraction profile for Nd_3RuO_7 at 10 K. The calculated and observed patterns are shown on the top solid line and the circles above the peaks, respectively. The vertical marks in the middle show positions calculated for Bragg reflections. The second vertical marks show the positions calculated for magnetic reflections due to Ru^{5+} ions. The lower trace is a plot of the difference between calculated and observed intensities.

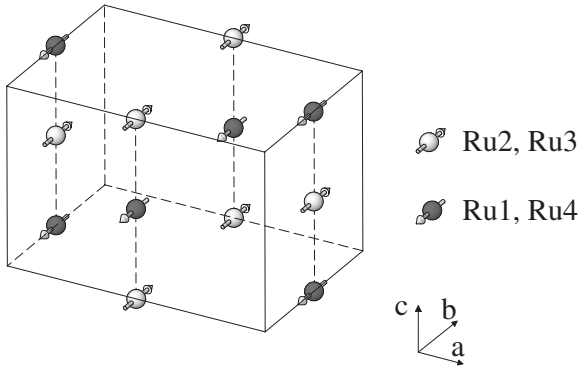

Figure 8. The magnetic structure of Nd_3RuO_7. Only ruthenium ions are depicted.

This coupling accords with that for La_3RuO_7 [3]. Refining the magnetic structure with the magnetic moments parallel to the *a*-, *b*- or *c*-axis, we can conclude that the directions of magnetic moments are parallel to the *b*-axis. The magnitude of the ordered magnetic moment is estimated to be 2.2 μ_B. This value is smaller than the saturated magnetic moment, 3 μ_B. Unfortunately, we could not determine the magnetic structure of Nd^{3+} sublattice because the magnetic reflections are too weak in intensity and because there are too many sites for the Nd^{3+} ions, 24 sites per magnetic unit cell.

Acknowledgment

This work was supported by Grant-in-aid for Science Research on Priority Area 'Novel Quantum Phenomena in Transition Metal Oxides—Spin Charge Orbital Couple Systems'

No 12046203 from the Ministry of Education, Science, Sports, and Culture of Japan. Thanks are also due to The Suhara Memorial Foundation.

References

[1] van Berkel F P F and IJdo D J W 1986 *Mater. Res. Bull.* **21** 1103
[2] Groen W A, van Berkel F P F and IJdo D J W 1987 *Acta Cryst.* C **43** 2262
[3] Khalifah P, Erwin R W, Lynn J W, Huang Q, Batlogg B and Cava R J 1999 *Phys. Rev.* B **60** 9573
[4] Khalifah P, Huang Q, Lynn J W, Erwin R W and Cava R J 2000 *Mater. Res. Bull.* **35** 1
[5] Wiss F, Raju N P, Wills A S and Greedan J E 2000 *Int. J. Inorg. Mater.* **2** 53
[6] Bontchev R P, Jacobson A J, Gospodinov M M, Skumryev V, Popov V N, Lorenz B, Meng R L, Litvinchuk and Iliev M N 2000 *Phys. Rev.* B **62** 12235
[7] Harada D and Hinatsu Y 2001 *J. Solid State Chem.* **158** 245
[8] Vente J F and IJdo D J 1991 *Mater. Res. Bull.* **26** 1255
[9] Kahn-Harari A, Mazerolles L, Michel D and Robert F 1995 *J. Solid State Chem.* **116** 103
[10] Greedan J E, Raju N P, Wegner A, Gougeon P and Padiou J 1997 *J. Solid State Chem.* **129** 320
[11] Morii Y 1992 *J. Cryst. Soc. Japan* **34** 62
[12] Izumi F and Ikeda T 2000 *Mater. Sci. Forum* **198** 321